some intermediate frequency range such as 100 to 200 Mc. The microwave signals can be detected by using the harmonics of the oscillator which are produced in the internal detector of the meter. Harmonics up to the twentieth can be used conveniently and reliably.[1]

The elements of a representative heterodyne frequency meter, intended for use between 10 to 3,000 Mc, are shown in Fig. 8.6. The variable-frequency oscillator, tuning from 100 to 200 Mc, is coupled to a crystal

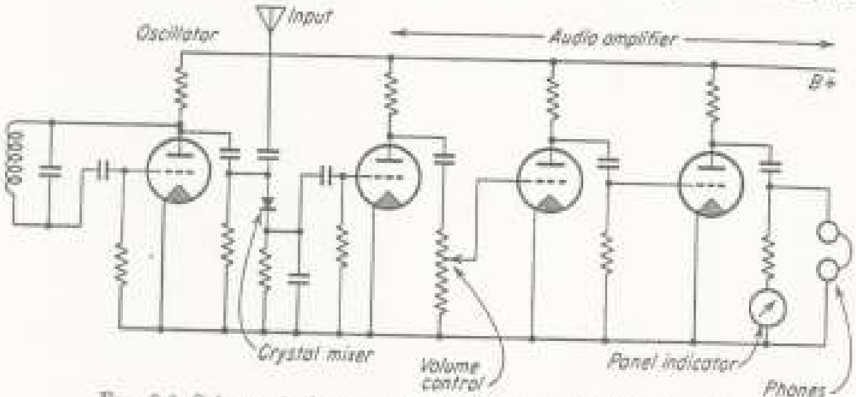

FIG. 8.6. Schematic diagram of the heterodyne frequency meter.

rectifier detector. The beat frequency is introduced into the audio amplifier, the output of which is available at either a panel meter or at terminals for use with head phones. The meter is used when the frequency is not sufficiently stable to produce steady, audible beat notes or the beat note is below an audible rate. The quartz-crystal oscillator can be connected to the input terminals for calibration. A 1-Mc quartz oscillator may be used to control a chain of multivibrators to generate low-frequency sequences. The 1-Mc crystal oscillator can be checked against WWV with the aid of a radio receiver.[2]

[1] One commercial model of a heterodyne frequency meter is described by E. Karplus, A Heterodyne Frequency Meter for 10 to 3,000 Megacycles, *General Radio Experimenter*, vol. 20, nos. 2 and 3, July and August, 1945.

[2] Details of operation of a heterodyne frequency meter can be found in an instruction book for the General Radio type 720-A heterodyne frequency meter. Several useful techniques of wide applicability are described.

GINZTON "MICROWAVE MEAS."

CHAPTER 9

RESONANT-CAVITY CHARACTERISTICS: MEASUREMENT OF Q

9.1. Introduction. At the low radio frequencies, the simple resonant circuit can be specified completely by stating the circuit parameters in terms of L, C, R_s as shown in Fig. 9.1. The equivalent description of the microwave resonant circuit cannot be so explicit because, as in the waveguide, the ordinary concept of voltage and current does not play its usual role. To define the circuit parameters in any microwave problem, it is necessary to select the set of field quantities that are of importance in the given application. Using these, the microwave circuit can be described in a manner that closely resembles low-frequency circuit practice. However, the microwave equivalent circuit concept is complicated by the relatively close spacing of the resonant frequencies of the microwave cavity. In most practical situations the cavities are used at sufficiently low frequencies that only one mode is excited at a time, thus making it possible to represent the energy stored in the fields of some particular mode by the energy stored in the lumped parameters of the equivalent circuit shown in Fig. 7.1. In the remaining material, it is assumed that this equivalent circuit accurately describes the observed physical phenomenon.[1]

A consideration of the low-frequency analogue clarifies the meaning of the equivalent circuit parameters. The three parameters shown in Fig. 9.1 can be related to the three universally useful relations:

$$\begin{aligned} \omega_0^2 &= \frac{1}{LC} \\ Q_0 &= \frac{\omega_0 L}{R_s} \\ R_0 &= \omega_0 L Q_0 \\ &= \frac{(\omega_0 L)^2}{R_s} \end{aligned} \tag{9.1}$$

[1] R. Beringer, chap. 7, in C. G. Montgomery, R. H. Dicke, and E. M. Purcell (eds.), "Principles of Microwave Circuits," vol. 8, Massachusetts Institute of Technology Radiation Laboratory Series, McGraw-Hill Book Company, Inc., New York, 1948.

The three quantities defined by these relations can be measured experimentally to provide the three relations needed to compute the three circuit parameters. If ω_0, Q_0, and R_0 are measured, the circuit parameters can be found by solving Eq. (9.1), resulting in

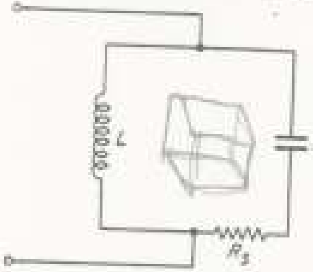

FIG. 9.1. Low-frequency resonance circuit.

$$L = \frac{R_0}{\omega_0 Q_0} \qquad C = \frac{Q_0}{\omega_0 R_0} \qquad R_s = \frac{R_0}{Q_0^2} \tag{9.2}$$

This procedure indicates how the three microwave circuit parameters can be evaluated from the experimental study of the resonant circuit as a whole.

The study of the microwave resonant cavity differs from that of the low-frequency circuit in two respects: first, the equivalent-circuit parameters must be established separately for each mode under consideration; and second, the quantity R_0, called the shunt resistance, is not uniquely defined due to the ambiguity in the meaning of the voltage and current. For convenience, R_0 can be defined as

$$R_0 = \frac{(\int \mathbf{E}\, dl)^2}{2(\text{power dissipated})} = \frac{(\int \mathbf{E}\, dl)^2}{2W} \tag{9.3}$$

where $\mathbf{E}$ is the peak electric field along the path of integration between some two points in the cavity and W is the power dissipated in the cavity.[1] For a few simple geometrical shapes the quantities ω_0, Q_0, and R_0 can be computed from the geometrical factors and the conductivity of the cavity walls. However, for most useful cavity shapes, mathematical computation is too difficult to be practical, and these quantities must be determined directly by experiment. Furthermore, both R_0 and Q_0 depend upon the particular sources of loss in the cavity and can be found only by experiment.

The knowledge of ω_0, Q_0, and R_0 is necessary and sufficient for the complete description of the resonant cavity in a given mode; in practice, these experimentally determined quantities form the set of cavity characteristics which are descriptive and sufficient for most applications. If necessary, the equivalent circuit parameters shown in Fig. 9.1 can be computed with the aid of Eq. (9.2).

[1] The choice of the definition of the shunt impedance on the basis of the power-voltage quantities is arbitrary. The impedance could also be defined on the basis of the voltage-current or current-power ratios, etc. As in the case of transmission-line problems, it can be shown that these definitions lead to different numerical results for the impedance, being the same only in special cases. The choice of the proper definition for a given problem depends upon the specific application. The particular definition stated above is useful in the class of problems in which one wishes to know the *axial electric field* in the cavity for a given *power dissipated* in the cavity. Specification of these quantities leads to a particular definition of impedance. It is useful in applications involving the interaction of electrons with the electric field in the cavity.

In Chap. 7 experimental procedures for the determination of the resonant frequency of the cavity are discussed in connection with the measurement of wavelength. The experimental techniques used to measure Q_0 are discussed in this chapter and those to determine R_0 in Chap. 10.

a. Equivalent Circuits; Definitions of Q_0, Q_L, Q_{ext}, and Coupling Coefficient β. A microwave cavity can be coupled to one, two, or more transmission lines. The cavity characteristics can be studied experimentally by measuring the self-impedance at one pair of input terminals, or by measuring the transfer of power from one set of terminals to another; the unused terminals, in either case, can be terminated in some known impedance. The complete description of the cavity characteristics and the effect of the coupled transmission lines can be evaluated by performing as many independent experiments as there are coupled transmission lines. By this process, the study of a cavity with multiple sets of input terminals can be reduced to the study of a system with only one or two sets of terminals.

The equivalent circuit of a cavity with two inputs is shown in Fig. 9.2. The coupling between the cavity and the transmission lines is symbolically represented by an iris which indicates some arbitrary method of exciting the cavity fields; it can be shown that the actual form of the coupling mechanism does not effect the equivalent circuit. The cavity resonance in a particular mode is represented by the parameters L, C, and R_s. Two alternate forms of the equivalent circuit representing the coupling between the circuit and the transmission lines are shown in Fig. 9.2*b* and *c*; in the first, the coupling is represented by ideal transformers and in the second, by mutual inductances. In general, the coupling between the cavity and the transmission lines contains both resistive and reactive components; for example, a coupling loop has both self-inductance and resistive loss. Irrespective of the details of the coupling mechanism, the inductances L_1 and L_2 represent the self-inductances of the coupling elements which are due to the fringing field caused by the geometrical discontinuity at the junction of the transmission line and the cavity. These equivalent circuits can be simplified for analysis by referring the impedances of the three circuit loops to a single one, as indicated in Fig. 9.2*d* and *e*.

The characteristic behavior of the complete system can be studied in several ways. The simplest is to observe the variation in the power delivered to the load as the frequency of the signal source is varied or

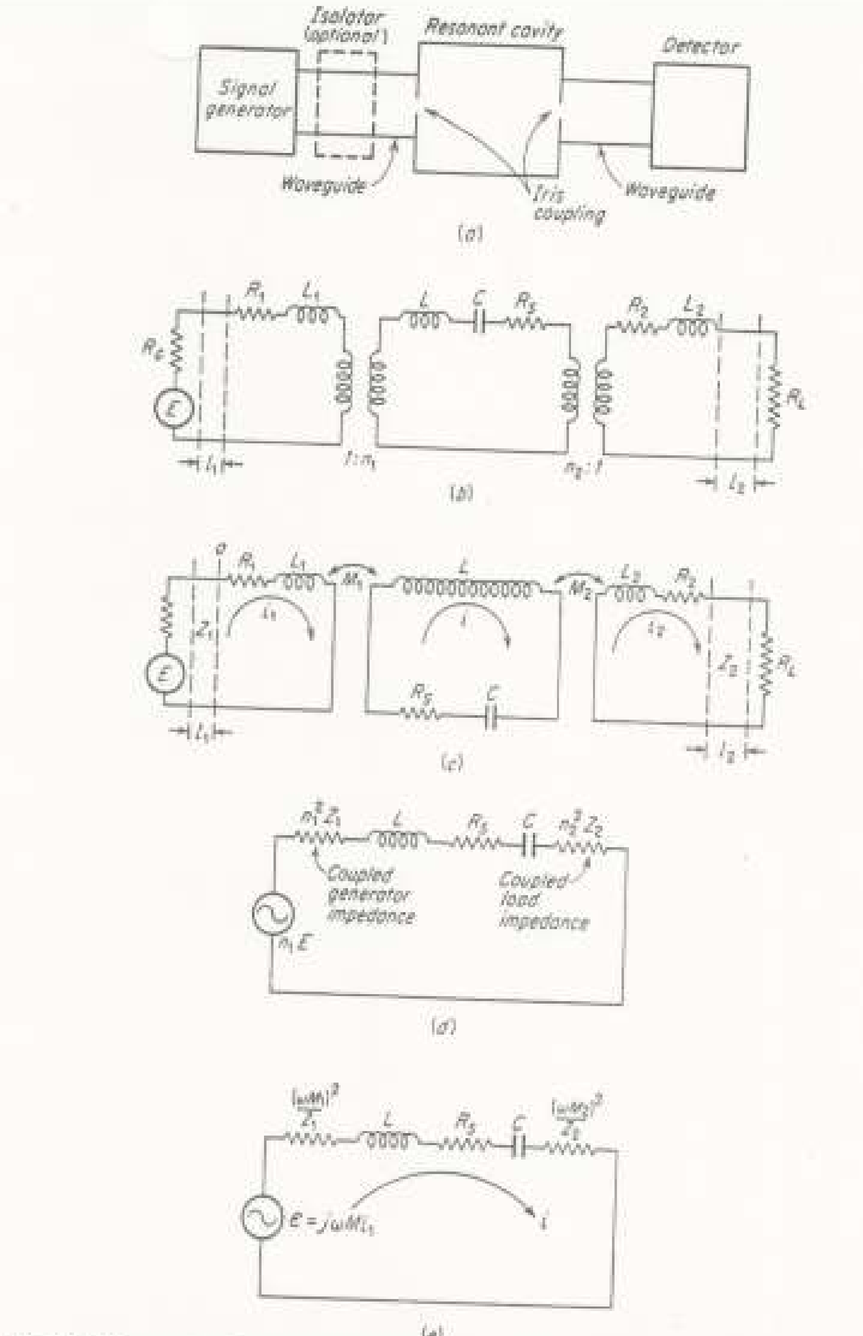

Fig. 9.2. Resonant cavity connected between a signal generator and a detector. (a) Symbolic representation using iris coupling to the waveguides; (b) the equivalent circuit using ideal transformers; (c) the equivalent circuit using mutual inductances; (d and e) the equivalent circuits referred to the middle loop, neglecting self-impedances of each side and assuming $R_G = Z_1$ and $R_L = Z_2$.

the cavity is tuned. In either case, the familiar resonance phenomenon occurs, causing the power output at resonance to differ substantially from the detuned condition. The exact behavior of the system depends upon the characteristics of the cavity and the degree of coupling between the cavity and the transmission lines.

Sometimes it is desired to measure the cavity parameters and the coefficients of coupling between the cavity and the transmission lines; sometimes it is merely desired to determine the unloaded cavity parameters, i.e., the characteristics of the cavity if it were not perturbed by the presence of the coupled transmission lines. For this purpose, it is convenient to measure the degree of coupling between the cavity and the transmission lines by specifying Q_0, Q_L, and Q_{ext}, the unloaded, the loaded, and the external Q values, respectively, as defined in Chap. 7. These definitions are important because applications occur in which the effective coupling is of primary importance and also because in any given measurement the effect of residual coupling must be known if the meaning of the measurements is to be properly interpreted.

For convenience, the definitions of the Q values given in Chap. 7 are repeated below. Consider a cavity coupled to a signal source whose internal impedance is equal to the characteristic impedance of the transmission line as indicated in Fig. 9.3a. The equivalent circuit of the cavity and the transmission line is shown in Fig. 9.3b, where the terminals of the coupling system (or network) are presumed to be located at some arbitrary position a-a near the cavity. L_1

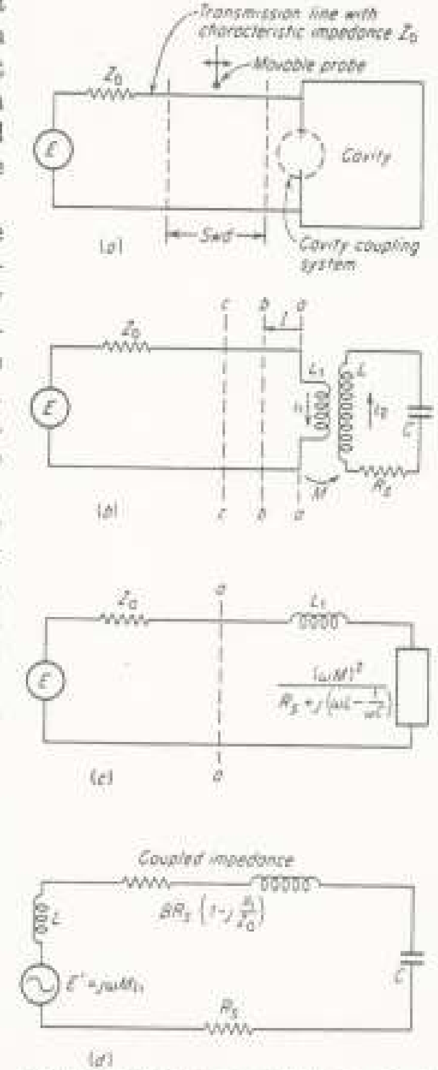

Fig. 9.3. Cavity coupled to a signal generator through a standing-wave detector. (a) The cavity-coupling system schematically; (b) the equivalent circuit; (c) the equivalent circuit with the impedances referred to the primary; (d) the equivalent circuit with the impedances referred to the secondary.

represent the self-inductance of the coupling mechanism and M the mutual inductance between it and the cavity inductance L. The resistive losses in the coupling network are neglected (the effect of dissipation in the coupling network is included in the analysis given in Sec. 9.4). This circuit can be simplified further as shown in Fig. 9.3c and d; in the first, the cavity is shown as a coupled impedance in series with the primary; in the second, the primary is represented as a coupled impedance in series with the cavity parameters. The impedance coupled in series with the cavity parameters due to a matched generator is given by

$$Z = \frac{(\omega M)^2}{Z_0 + j\omega L_1} \tag{9.4}$$

$$= \frac{(\omega M)^2}{Z_0[1 + (\omega L_1/Z_0)^2]}\left(1 - j\frac{\omega L_1}{Z_0}\right) \tag{9.5}$$

Using definitions given by Eqs. (9.11) and (9.12), and $X_1 = \omega L_1$, Eq. (9.5) becomes

$$Z = \beta R_s\left(1 - \frac{jX_1}{Z_0}\right) \tag{9.6}$$

The *loaded* Q value of the system is defined as the ratio of total reactance to total series loss. It is given by

377.18

$$Q_L = \frac{\omega L - \beta R_s X_1/Z_0}{R_s(1+\beta)} \tag{9.7}$$

$$= \frac{\omega L}{R_s}\,\frac{1 - (\beta R_s/Z_0)(X_1/\omega L)}{1+\beta} \tag{9.8}$$

The second term in the numerator of Eq. (9.8), representing the ratio of coupled reactance to the cavity reactance, is usually small compared to unity and can be neglected. Equation (9.8) then becomes

$$\boxed{Q_L = \frac{Q_0}{1+\beta}} \qquad (\beta+1)Q_L = Q_0 \tag{9.9}$$

where

$$Q_0 = \frac{\omega L}{R_s} \qquad \Rightarrow Q_L = \frac{Q_0}{1+A\cdot X^2} \tag{9.10}$$

$\beta = X^2$

$$\beta = \frac{(\omega M)^2}{Z_0 R_s}\,\frac{1}{1 + (X_1/Z_0)^2} \tag{9.11}$$

$$= \beta_1 \frac{1}{1 + (X_1/Z_0)^2} \qquad \beta \to 0 \;\Rightarrow Q_L \to Q_0 \tag{9.12}$$

where $\beta_1 = (\omega M)^2/Z_0 R_s$ is the ratio of the coupled resistance to the cavity resistance R_s. When $\beta_1 = 1$, the coupled resistance and cavity losses are equal, and the cavity is said to be *critically* coupled. When $\beta_1 < 1$, the cavity is said to be *undercoupled;* when $\beta_1 > 1$, the cavity is called *overcoupled.* Under most circumstances, the second term in Eq. (9.12) is nearly equal to unity and $\beta \approx \beta_1$. Thus, at critical coupling $Q_L \approx Q_0/2$.

Equation (9.9) can be written as

$$\frac{1}{Q_L} = \frac{1}{Q_0} + \frac{\beta}{Q_0} \tag{9.13}$$

or

$$\frac{1}{Q_L} = \frac{1}{Q_0} + \frac{1}{Q_{ext}} \tag{9.14}$$

where

$$Q_{ext} = \frac{Q_0}{\beta} \tag{9.15}$$

or

$$\beta = \frac{Q_0}{Q_{ext}} \tag{9.16}$$

b. Q Circles. The solution of many problems involving resonant cavities can be simplified by considering, either graphically or analytically, the cavity input impedance in the complex impedance plane.

The impedance at the terminals of the coupling network *a-a* in Fig. 9.3b is equal to

$$Z_{aa} = jX_1 + \frac{(\omega M)^2}{R_s + j(\omega L - 1/\omega C)} \tag{9.17}$$

or

$$\frac{Z_{aa}}{Z_0} = j\frac{X_1}{Z_0} + \frac{\beta_1}{1 + j(\omega L/R_s)[1 - (\omega_0/\omega)^2]} \tag{9.18}$$

where $\omega_0^2 = 1/LC$. For cavities with high Q_0, $\omega \approx \omega_0$. Equation (9.18) can then be written as

$$\boxed{\frac{Z_{aa}}{Z_0} = j\frac{X_1}{Z_0} + \frac{\beta_1}{1 + j2Q_0\delta}} \tag{9.19}$$

where

$$\delta = \frac{\omega - \omega_0}{\omega} \tag{9.20}$$

The quantity δ is called the *frequency-tuning parameter.* For high-Q systems, δ can be considered to be the variable, irrespective of whether the frequency of the signal ω or the resonant frequency of the cavity ω_0 is changed.

Consider a plot of Eq. (9.19) in the rectangular impedance plane. The second term of this equation corresponds to an equation of a circle, representing the impedance of a shunt resonance circuit with a resonant impedance $\beta_1 Z_0$. The effect of the self-reactance of the coupling system, as expressed by the first term in Eq. (9.19) is to displace the circle along the imaginary axis, as indicated in Fig. 9.4a.

The analysis and interpretation of certain experiments can be aided by choosing special reference planes along the transmission line at which the term representing the self-reactance of the coupling system disappears. This happens at a series of singular locations, half a wavelength apart, which are called the *detuned-short* positions. At frequencies

$\delta >> 1$

far off resonance, the second term in Eq. (9.19) vanishes, leaving the self-reactance of the coupling system as the terminating load. This reactive termination produces a complete reflection of the incident signal and results in a series of voltage nodes which can be found by means of the standing-wave detector.

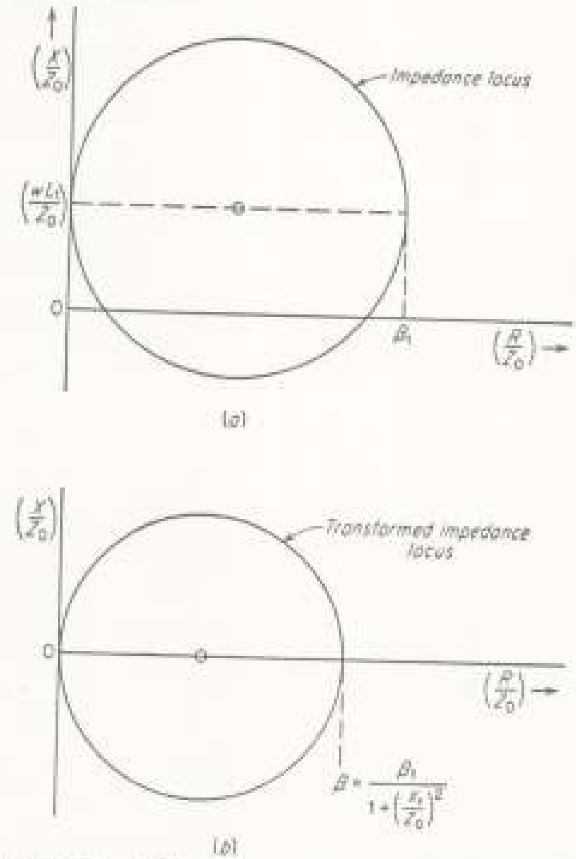

FIG. 9.4. Input impedance of the resonant cavity. (a) The impedance referred to some arbitrary position near the cavity; (b) the impedance locus referred to the detuned short position. (self-reactance $\frac{X_1}{Z_0}$

The impedance at the detuned short position, looking toward the cavity, is especially simple, having the form of a simple resonant shunt circuit. This can be demonstrated analytically as follows: Let the terminals b-b be selected at a distance l away from the terminals a-a.*

* The arbitrary choice of the original terminals at a-a determines the effective value of the coupling reactance L_1. In practice, the exact location of the terminals a-a is of no concern because all of the quantities can be referred directly to the unambiguous location of the detuned short.

Using Eq. (4.64), the cavity impedance at a-a can be transformed to the terminals b-b.* Therefore,

$$\frac{Z_{bb}}{Z_0} = \frac{Z_{aa} + jZ_0 \tan \beta l}{Z_0 + jZ_{aa} \tan \beta l} \tag{9.21}$$

The location of the terminals b-b can be chosen so that the impedance at terminals b-b becomes zero when the cavity is detuned.

With the cavity detuned, $Z_{aa} = jX_1$. Hence, $Z_{bb} = 0$ when

$$\tan \beta l = -\frac{X_1}{Z_0} \tag{9.22}$$

or (not β coupling)

$$\beta l = -\tan^{-1}\left(\frac{X_1}{Z_0}\right) \tag{9.23}$$

Combining Eqs. (9.19), (9.21), and (9.23), the impedance at the detuned short position for any value of δ becomes

$$\frac{Z_{bb}}{Z_0} = \frac{\beta}{1 + j2Q_0(\delta - \delta_0)} \tag{9.24}$$

coupling

where

$$\delta_0 = \frac{\beta}{2Q_0}\left(\frac{X_1}{Z_0}\right) \tag{9.25}$$

Equation (9.24) represents the impedance of a parallel resonant circuit with a resonant impedance βZ_0; a graph of this location in the impedance plane is shown in Fig. 9.4b. A comparison of Eqs. (9.19) and (9.24) shows that the diameter of the resultant transformed circle is different from the one that corresponds to the impedance at a-a. Also, the resonant frequency of the circuit described by Eq. (9.24) no longer occurs at the natural resonant frequency of the cavity but is altered by the amount given by Eq. (9.25). However, these changes are not especially significant and can be taken into account in the interpretation of the results.

The shunt representation can be transformed into a series representation if the reference plane is chosen $\lambda_l/4$ away from the detuned-short position. This position can be termed the *detuned-open* position. Transforming Eq. (9.24) through $\lambda_l/4$ with the aid of Eq. (4.64) leads to

$$\frac{Z_{cc}}{Z_0} = \frac{1}{\beta}[1 + j2Q_0(\delta - \delta_0)] \tag{9.26}$$

This is an equation of a series resonant circuit; the impedance at resonance is Z_0/β. Both the shunt and series representations are indicated in Fig. 9.5.

* Unfortunately, the symbol β has two different meanings in the following equations. When used in the expression $\tan \beta l$ it represents the *propagation constant* in the transmission line; when β is used alone, the meaning is the principal one in this chapter, i.e., the *coupling coefficient*.

c. Typ. , Q Measurements. The Q values of a resonant cavity can be determined experimentally in many ways. These can be divided into four groups:

1. Transmission method
2. Impedance measurement
3. Transient decay or the decrement method
4. Dynamic methods

In the first of these, the cavity with input and output terminals is used as a transmission device. The output signal is measured as a func-

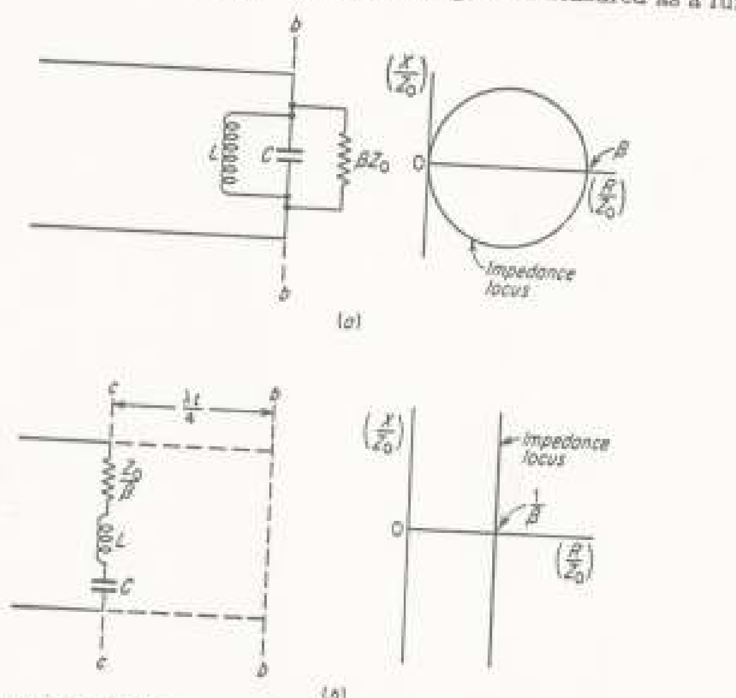

FIG. 9.5. Shunt and series representation of the resonant cavity: The equivalent impedance (a) at the detuned-short position, (b) at the detuned-open position. The corresponding loci are shown in the complex impedance plane.

tion of frequency, resulting in the conventional resonance curve from whose bandwidth the Q value can be computed. Although it is simple conceptually, there are practical difficulties in its application which make it necessary to pay considerable attention to several details to obtain accurate results. The use of this method is described in Sec. 9.2.

The second method, discussed in Sec. 9.3, is based upon the observation of the variation of the cavity input impedance with frequency. If the impedance of the cavity is measured as a function of frequency,

the impedance locus referred to the detuned-short position will lie on a circle; if referred to the detuned-open position, the locus will lie on a straight line. These data can be readily interpreted to provide the values of Q_0, Q_L, and Q_{ext}. Since a circle can be defined by three points, it is necessary to make only three independent impedance measurements to describe completely the characteristics of the cavity and its coupling system. To improve the accuracy, additional data are usually taken to detect random, systematic, or accidental errors.

The impedance data can be interpreted by one of several methods. The standing-wave ratio can be used alone without the corresponding phase data. A plot of VSWR versus frequency contains all the necessary information; the use of this data is analogous to employing the universal resonance curve of a resonant circuit at low frequencies. Conversely, the phase data can be used without the VSWR data. The detailed discussion of these methods shows that sometimes one can choose between these methods in accordance with his preference. Sometimes, however, the choice of a particular method can lead to greater accuracy. Consider, for example, the Smith chart plot shown in Fig. 9.6 of the input impedance for three degrees of coupling.

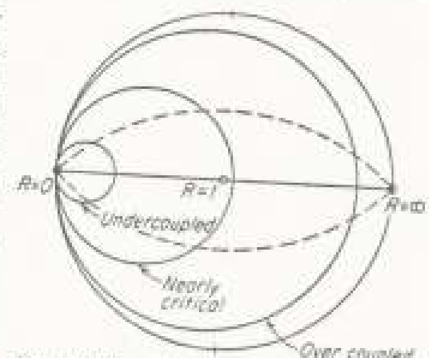

FIG. 9.6. Input impedance of a resonant cavity referred to the detuned-short position plotted in the Smith chart for three degrees of coupling.

If the cavity is nearly critically coupled, the circle passes through the real axis near the point (1,0). In this case, both the VSWR and the phase information are equally important; the best accuracy is obtained for measuring the vector impedance at each frequency. If, however, the cavity is weakly coupled ($\beta \ll 1$), the resultant impedance locus is a very small circle. In this case, the phase data are not accurate because the entire circle is contained within a small range of phase angles. However, the VSWR varies substantially with frequency and the determination of the frequency interval between certain "half-power points" results in good accuracy. If the cavity is greatly overcoupled ($\beta \gg 1$), the resultant circle approaches the periphery of the Smith chart; the VSWR is high and does not change appreciably, but the phase angle changes rapidly and provides the needed information.

The decrement method described in Sec. 9.5, particularly applicable to high-Q cavities, uses the transient decay of the natural oscillations in the cavity. If the cavity under study is excited by a pulsed signal, during the off pe. the natural fields in the cavity decay exponentially with time and the time constant of the decay determines the Q. Figure 9.7a shows the equipment necessary for this method. A pulsed-modulated oscillator provides signals of sufficient duration to establish steady-state fields in the cavity. The output signal from the cavity is detected by a sensitive detector (preferably, a superheterodyne receiver), amplified by

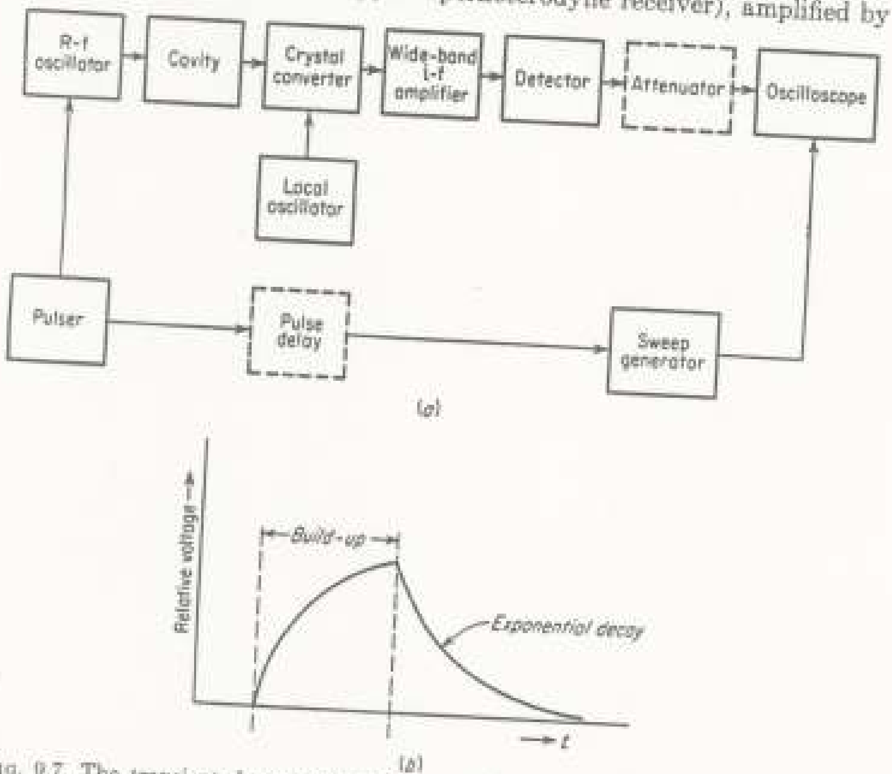

FIG. 9.7. The transient decay method of measuring the Q value. (a) The typical equipment, with dashed rectangles indicating optional equipment; (b) the transient build-up and decay observed on the oscilloscope.

a wideband amplifier, and observed by an oscilloscope whose sweep is synchronized by the pulser. The typical response is indicated in Fig. 9.7b. The time constant is measured and the results interpreted as described in Sec. 9.5.

The decrement method is especially convenient for the high-Q systems because it does not need the high degree of frequency stability required in other types of measurements. This is apparent from the fact that in other methods the frequency must be sufficiently stable during the course of a given measurement; for example, in using VSWR measurements, the frequency must be constant at least during the time needed to measure

a single standing-wave ratio. The measurement of Q values in excess of 10^4 is especially simple; however, at lower values, the decay period is too short for convenient measurement.

The fourth group of methods described in Sec. 9.6 is based upon the dynamic observation of the cavity characteristics. These techniques are useful for two reasons: the frequency stability requirements of the signal

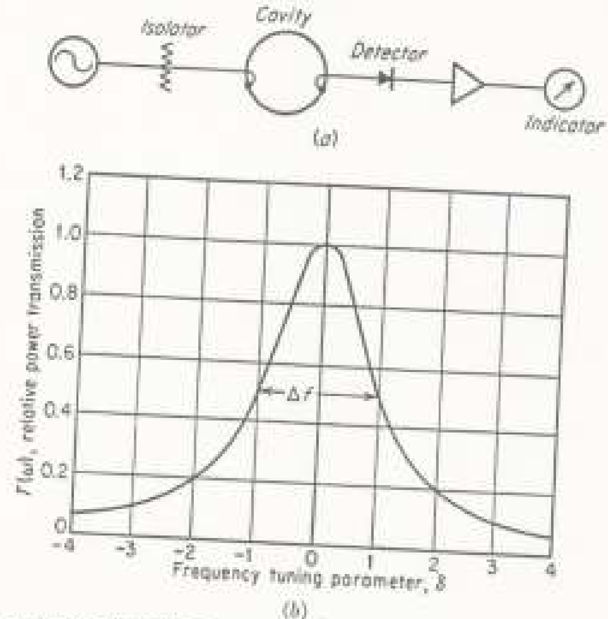

FIG. 9.8. Transmission method of measuring the Q value. (a) The equipment used; (b) the typical transmission curve.

source are reduced; and the Q values can be obtained more quickly, sometimes from a direct reading meter.

9.2. Transmission Method. The transmission method illustrated in Fig. 9.8a is the simplest phenomenological measurement of Q. A signal generator, preferably completely isolated from the load by a resistive pad or a ferrite isolator, is connected to the cavity through the input coupling system; a detector with a known response low is connected to the output coupling system. By varying the frequency of the signal generator, the transmission resonance curve shown in Fig. 9.8b can be observed from whose bandwidth the cavity Q can be determined. The resonance curve can be obtained also by tuning the cavity and keeping the frequency of the oscillator fixed. A choice between the two methods depends upon the details and ease of tuning and calibrating the apparatus under test.

The relation between the observed bandwidth of the resonance curve, the input and output coupling coefficients, Q_0, and Q_L can be obtained as follows: Assume that the load and generator impedances indicated in Fig. 9.2b are equal to the characteristic impedances of their respective lines. The losses of the coupling systems represented by R_1 and R_2 can be neglected or considered as parts of R_G and R_L, respectively. The self-inductances L_1 and L_2 can also be neglected; this approximation changes slightly the apparent resonant frequency of the system but for high-Q systems does not have other effects. With these approximations, Fig. 9.2b can be altered by referring both the primary and the tertiary loops into the middle loop, which results in the equivalent circuits shown in Fig. 9.2d and e. The loaded Q of the system is

$$Q_L = \frac{\omega_0 L}{R_s + n_1^2 Z_1 + n_2^2 Z_2} \tag{9.27}$$

or

$$Q_L = \frac{\omega_0 L}{R_s + (\omega M_1)^2/Z_1 + (\omega M)^2/Z_2} \tag{9.28}$$

where Z_1 and Z_2 represent the characteristic impedances of the input and output transmission lines, respectively. The input and output coupling coefficients are defined as

$$\beta_1 = n_1^2 \frac{Z_1}{R_s} = \frac{(\omega M_1)^2}{R_s Z_1} \tag{9.29}$$

$$\beta_2 = n_2^2 \frac{Z_2}{R_s} = \frac{(\omega M_2)^2}{R_s Z_2} \tag{9.30}$$

Using these, the relation between Q_0 and Q_L becomes

$$Q_0 = Q_L(1 + \beta_1 + \beta_2) \tag{9.31}$$

The relation between the width of the resonance curve and the cavity Q is obtained as follows: The *transmission loss* $T(\omega)$ through the cavity is defined as

$$T(\omega) = \frac{P_L}{P_0} \tag{9.32}$$

where P_L is the power delivered to a load and P_0 is the maximum power available from the generator (to a matched load). Computing P_L and P_0 for Fig. 9.2d,

$$T(\omega) = \frac{4\beta_1\beta_2}{(1 + \beta_1 + \beta_2)^2 + 4Q_0^2\delta^2} \tag{9.33}$$

where δ is the tuning parameter defined in Eq. (9.20). At resonance $\delta = 0$, and Eq. (9.33) becomes

$$T(\omega_0) = \frac{4\beta_1\beta_2}{(1 + \beta_1 + \beta_2)^2} \tag{9.34}$$

Dividing Eq. (9.33) by Eq. (9.34), and using Eq. (9.31),

$$T(\omega) = \frac{T(\omega_0)}{1 + 4Q_L^2\delta^2} \tag{9.35}$$

The *half-power* points of transmission occur when

$$2Q_L\delta = \pm 1 \tag{9.36}$$

or

$$2\delta = \pm \frac{1}{Q_L} \tag{9.37}$$

or

$$2\delta = \pm \frac{1 + \beta_1 + \beta_2}{Q_0} \tag{9.38}$$

The quantity Δf is known as the *half-power bandwidth* of the resonance curve and is given by

$$\frac{\Delta f}{f} = 2\delta \tag{9.39}$$

Hence,

$$Q_0 = \frac{f}{\Delta f}(1 + \beta_1 + \beta_2) \tag{9.40}$$

Thus, if the signal generator and detector impedances are both matched, the measured transmission curve shown determines Q_L. The unloaded Q can be calculated if the coupling coefficients can be measured separately. However, the greatest value of the procedure lies in finding Q_0 by reducing the coupling coefficients sufficiently. This is usually done by reducing the coupling between detector and the cavity until it is found that further reduction in coupling no longer affects the measured resonance curve. A separate experiment must also be carried out to assure that the coupling between the cavity and the signal generator is sufficiently small. Depending upon practical circumstances, these procedures can be either simple or complicated. For example, if the coupling systems consist of inductive coupling loops, adjustable by rotation or withdrawal, the coupling coefficients can be reduced readily. If the coupling is provided by means of an iris, such procedures are generally impractical.

The transmission method suffers from the fact that a single measurement of the transmission curve alone, no matter how accurately made, does not give the Q values directly. For this reason, the unambiguous procedures involving the measurement of impedance, described in Sec. 9.3, are more commonly used. However, the transmission method, if carefully executed, is capable of producing good accuracy. It should be noted that the presence of loss in the coupling systems is not important, which is not the case in the impedance methods.

9.3. The Impedance Method. As explained in Sec. 9.1b, the cavity characteristics can be determined by measuring the input impedance of a cavity a function of frequency. The details of this method are considered in this section in several forms.

In Sec. 9.3*a*, procedures for determining the Q parameters are described for those conditions of coupling which permit accurate measurement of the impedance with frequency. If the coupling coefficient is very small, corresponding to the high values of Q_L, the standing-wave ratio alone can be measured, a procedure described in Sec. 9.3*b*. When the coupling coefficient is large compared to unity, corresponding to low values of Q_L, the phase of the input impedance becomes more meaningful and can be used independently as described in Sec. 9.3*c*.

The choice of the most appropriate method in a particular application is a matter of convenience, experience, and personal preference as there is no obvious division between the usefulness of the three methods mentioned. In some cases, a combination is more convenient; for example, the phase data can be used more readily if the standing-wave ratio at resonance is measured also. However, experience with the basic methods is most helpful in deciding upon the value of possible variations.

In the discussion of the basic methods the effect of loss in the coupling system is neglected; this is justified in nearly all cases. The more general case is discussed in Sec. 9.4 where this assumption is avoided.

a. Interpretation of the Impedance Data. The impedance method is used as follows. Figure 9.3 shows the cavity under study connected to a uniform transmission line through its cavity coupling system. A standing-wave detector is placed between the signal generator and the cavity to measure the input impedance. The measurement procedures are simplified if the relative tuning of the cavity and the signal generator are independent, i.e., if cavity tuning does not affect the output of the signal generator. It is particularly convenient to have the impedance of the signal source equal to Z_0.

The procedure begins with the determination of the detuned short position. The signal frequency is adjusted to the desired value and the cavity is detuned completely; this effectively terminates the transmission line in a pure reactance. The standing-wave detector is used to find a voltage node which locates the detuned short position; this location is recorded for future use (for convenience it can be marked on the standing-wave detector with a pencil). If the cavity is not tunable, the equivalent experiment can be performed by tuning the signal generator sufficiently far from the resonant frequency of the cavity. For high-Q systems, the change in frequency is not large, and the location of the detuned short determined in this manner is nearly the correct one. It is the approximate but not quite the correct value, as can be seen from Eq. (9.23). In case of doubt, it may be necessary to plot the position of the detuned short as a function of frequency and to refer further impedance measurements to a detuned short position appropriate for the particular frequency.

Next, it is necessary to determine the magnitude of the coupling coefficient, as the choice among the possible techniques depends upon its value. The probe of the standing-wave detector is placed at the detuned short position; Figure 9.5*a* shows that this locates the probe across the terminals of an equivalent-shunt resonant circuit. Tuning the cavity to produce the maximum voltage in the probe is equivalent to tuning the cavity to resonance, *provided* the source impedance is purely resistive. If this procedure is carried out correctly, the motion of the probe with respect to the detuned-short position will result in *either* a voltage maximum or voltage minimum at the detuned-short position since the cavity at resonance is a pure resistance. If the exploration of the standing-wave pattern results in a voltage minimum, the cavity is undercoupled; if it produces a maximum, the cavity is overcoupled. If the exploration indicates that a minimum (or a maximum) is not at the detuned-short position, some adjustment has been executed incorrectly. Assuming that the detuned-short position is located correctly, this means that the cavity is not exactly tuned to resonance, which is most likely if the source impedance is not purely resistive. The correct cavity tuning for resonance can be found by trial until either a minimum or a maximum occurs exactly at the detuned-short position.

The magnitude of the coupling coefficient is obtained by measuring VSWR at resonance. Since the impedances at the voltage minimum and maximum are Z_0/r_0 and Z_0r_0, respectively, where r_0 is the value of VSWR at resonance, Eq. (9.24) results in

Undercoupled case:
$$\beta = \frac{1}{r_0} \tag{9.41}$$

Overcoupled case:
$$\beta = r_0 \tag{9.42}$$

The evaluation of β locates the intersection of the impedance circle with the real axis in an impedance plot shown in Fig. 9.6.

If the coupling coefficient β is not greatly different from unity, the cavity tuning parameter δ can be changed in small increments and the impedance measured at each frequency. Typical experimental data are shown plotted in Figs. 9.9*a* and 9.9*b*; the first shows the impedance referred to the detuned-short position, and the second, to the detuned-open position.

Referring to Eq. (9.24), at certain frequencies the imaginary part of the denominator becomes equal to ± 1. At these values of δ, the input impedance becomes

$$\frac{Z_{bb}}{Z_0} = \frac{\beta}{1 \pm j} \tag{9.43}$$

The locus of these points (corresponding to $R = X$) for all possible values of β shown in Fig. 9.10 is a circle with the center on the periphery of the Smith chart at 90° points and passes through the two endpoints of the resistive axis. The intersection of this circle with the circle representing the graph of the impedance as a function of frequency determines

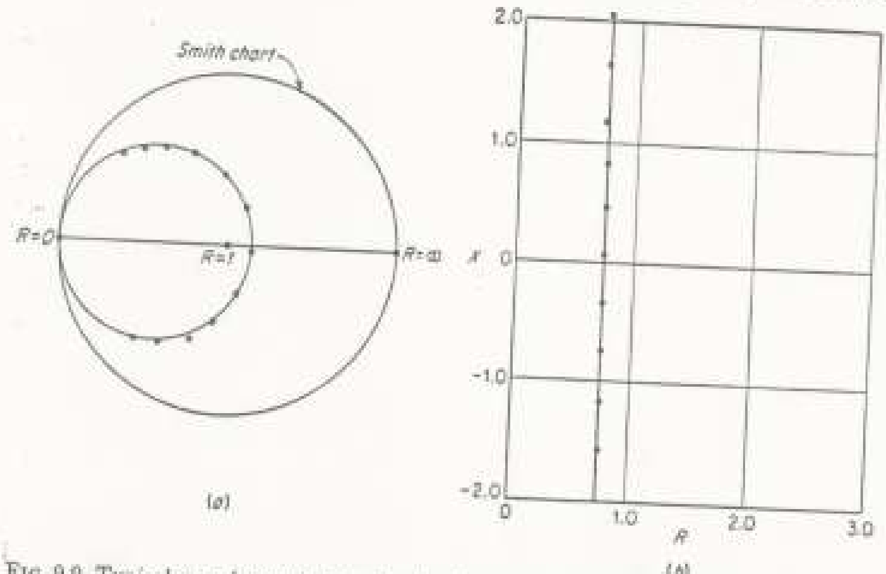

FIG. 9.9. Typical experimental data showing the variation of the input impedance of a resonant cavity with frequency. Impedance referred (a) to the detuned-short position, (b) to the detuned-open position. Data obtained for $f_0 = 3{,}000$ Mc, $Q_0 = 2{,}180$, $\beta = 1.31$.

those frequencies at which

$$2Q_0(\delta - \delta_0) = \pm 1 \tag{9.44}$$

Let these two values of δ be called δ_1 and δ_2. Hence,

$$\begin{aligned} 2Q_0(\delta_1 - \delta_0) &= 1 \\ 2Q_0(\delta_2 - \delta_0) &= -1 \end{aligned} \tag{9.45}$$

Subtracting and rearranging,

$$Q_0 = \frac{1}{\delta_1 - \delta_2} \tag{9.46}$$

or, in terms of frequency,

$$Q_0 = \frac{f_0}{f_1 - f_2} = \frac{f}{\Delta f} \tag{9.47}$$

Thus, the two frequencies at which the impedance locus passes through the points $R = X$ determine the unloaded Q value. Frequencies f_1 and f_2 are called the *half-power points.*

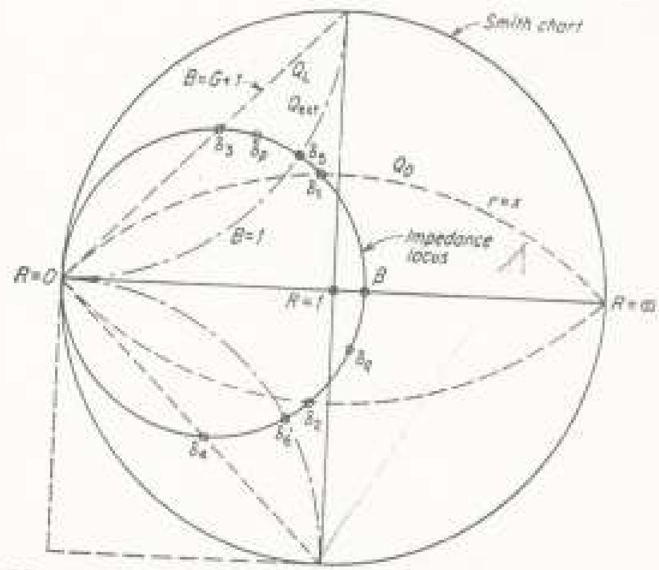

FIG. 9.10. Identification of the half-power points from the Smith chart. Q_0 locus is given by $X = R(B + G)$; Q_L by $B = G + 1$; Q_{ext} by $B = 1$.

The loaded and external Q values can be determined as follows: These are related to Q_0 through Eqs. (9.9) and (9.16). In terms of Q_L, Eq. (9.24) becomes

$$\frac{Z_{in}}{Z_0} = \frac{\beta}{1 + j2Q_L(1 + \beta)(\delta - \delta_0)} \tag{9.48}$$

In terms of Q_{ext},

$$\frac{Z_{in}}{Z_0} = \frac{\beta}{1 + j2Q_{ext}\beta(\delta - \delta_0)} \tag{9.49}$$

Let δ_3 and δ_4 be the tuning parameters at which

$$2Q_L(\delta - \delta_0) = \pm 1 \tag{9.50}$$

and δ_5 and δ_6 the tuning parameters at which

$$2Q_{ext}(\delta - \delta_0) = \pm 1 \tag{9.51}$$

From these it is found, in a manner analogous to the derivation of Eq. (9.47), that

$$Q_L = \frac{1}{\delta_3 - \delta_4} \tag{9.52}$$

$$Q_{ext} = \frac{1}{\delta_5 - \delta_6} \tag{9.53}$$

By using the conditions given by Eqs. (9.50) and (9.51) the values of these tuning parameters can be identified from the graph of impedance plot with the aid of Eqs. (9.48) and (9.49). From these, the locus of points determining Q_L is given by

$$\frac{Z_{bb}}{Z_0} = \frac{\beta}{1 \pm j(1+\beta)} \tag{9.54}$$

The locus of points giving Q_{ext} is given by

$$\frac{Z_{bb}}{Z_0} = \frac{\beta}{1 \pm j\beta} \tag{9.55}$$

These remarks are summarized in Fig. 9.10, which shows the location of the half-power points corresponding to Q_0, Q_L, and Q_{ext} with the aid of the defining loci given by Eqs. (9.43), (9.54), and (9.55).

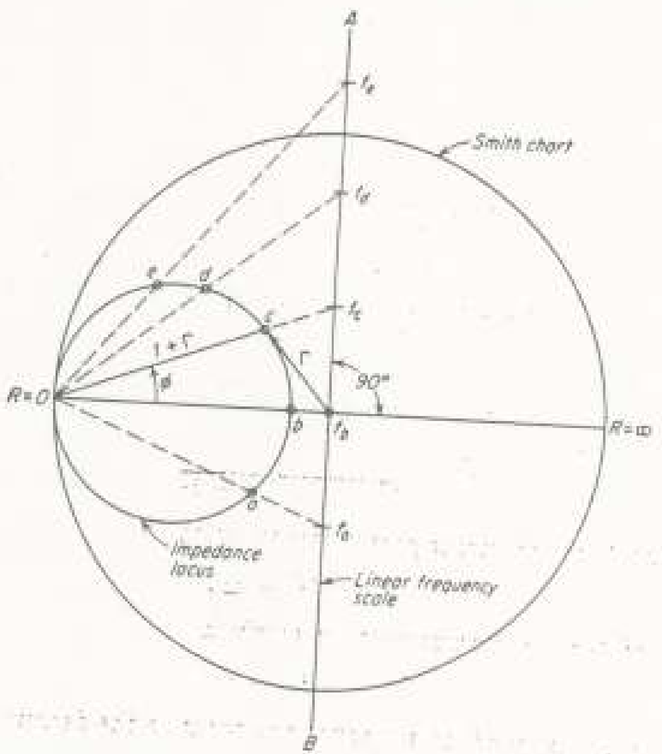

FIG. 9.11. Geometrical construction used to establish a linear frequency scale for the Q-circle impedance locus.

The distribution of the measured points along the circular locus in the Smith chart is not linear with frequency; this makes impossible the accurate determination of the frequencies corresponding to the half-power points by interpolation between the measured points. An auxiliary scale of linear frequency, helpful in avoiding this difficulty, can be established

by the construction shown in Fig. 9.11. The line AB is drawn perpendicularly to the resistive axis at any convenient location. The experimental impedance points such as a, b, c, d, and e, corresponding to the frequencies f_a, f_b, f_c, f_d, and f_e, respectively, are plotted. These points are projected upon the auxiliary frequency scale as indicated.[1] Thus, the frequency of any point on the impedance locus whose frequency is not known can be found by projecting it to the frequency scale.

The Q values can be obtained also from the rectangular impedance chart shown in Fig. 9.12. The derivation of the defining loci for the three Q values is obtained as above, using Eq. (9.26) in place of Eq. (9.24). The use of the rectangular impedance chart is often advantageous because:

1. All loci are straight lines, which permits simple graphing.
2. The frequency scale along the impedance locus is linear.
3. The frequency scale along the impedance locus is independent of the position of the locus in the impedance plane.
4. The half-power points identifying the tuning parameters corresponding to Q_0, Q_L, and Q_{ext} are found at the intersection of the straight lines.
5. The change of the cavity Q, due to changes in loading, displaces the impedance locus horizontally.

It is not necessary to use the half-power points to find Q values. A knowledge of the wavelength λ_t and two impedances, measured at two arbitrary values of δ, is sufficient to provide the necessary information. Consider, for example, points δ_p and δ_q shown in Figs. 9.10 and 9.12. If the laboratory data are plotted on the Smith chart, the resistance and

[1] The construction used in Fig. 9.11 can be proved as follows: The reflection coefficient Γ corresponding to the impedance given by Eq. (9.24) can be computed from

$$\Gamma = \frac{Z_{bb}/Z_0 - 1}{Z_{bb}/Z_0 + 1} \tag{9.56}$$

$$= \frac{\beta - [1 + j2Q(\delta - \delta_0)]}{\beta + [1 + j2Q(\delta - \delta_0)]} \tag{9.57}$$

$$= -1 + \frac{2\beta}{\beta + 1 + j2Q(\delta - \delta_0)} \tag{9.58}$$

or

$$\Gamma + 1 = \frac{2\beta}{\beta + 1 + j2Q(\delta - \delta_0)} \tag{9.59}$$

The phase angle ϕ of the radius vector originating from the origin (O,O) in Fig. 9.11 is equal to the phase angle of the vector $(1 + \Gamma)$. Hence,

$$\phi = \arg(\Gamma + 1) \tag{9.60}$$

$$= \tan^{-1} \frac{2Q(\delta - \delta_0)}{\beta + 1} \tag{9.61}$$

Therefore, the intercept along the axis AB, being proportional to $\tan \phi$, is proportional to the frequency.

reactance components of the impedances can be obtained directly from the chart coordinates. [Alternately, they can be computed from the measured VSWR and the position of the minimum using Eq. (4.78).]

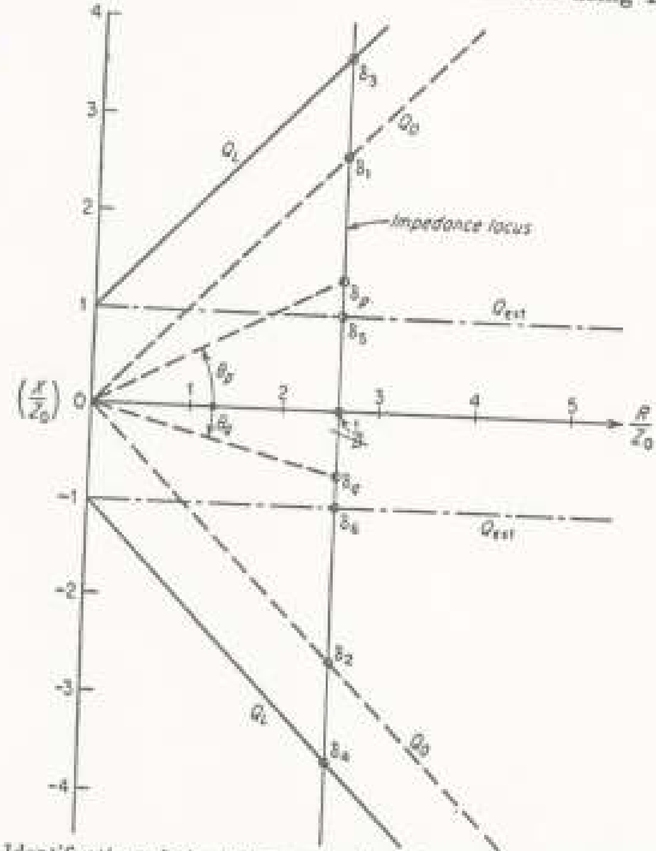

FIG. 9.12. Identification of the half-power points from the rectangular impedance chart.

If X and R are the imaginary and the real parts of the impedance given by Eq. (9.24), the ratios X/R for δ_p and δ_q are

$$\left(\frac{X}{R}\right)_q = -2Q_0(\delta_q - \delta_0)$$
$$\left(\frac{X}{R}\right)_p = -2Q_0(\delta_p - \delta_0) \qquad (9.62)$$

Subtracting and rearranging,

$$Q_0 = \frac{1}{2}\frac{1}{\delta_p - \delta_q}\left[\left(\frac{X}{R}\right)_q - \left(\frac{X}{R}\right)_p\right] \qquad (9.63)$$

which reduces to Eqs. (9.46) and (9.47) if $(X/R)_p = 1$, and $(X/R)_p = -1$.

If the laboratory data are plotted in the rectangular coordinates, as shown in Fig. 9.12, the quantity X/R is recognized as the angle θ of the radius vector to a point on the impedance locus. Thus, if $\tan\theta_p = (X/R)_p$, $\tan\theta_q = (X/R)_q$, using Eq. (9.62),

$$Q_0 = \frac{1}{2}\frac{1}{\delta_p - \delta_q}(\tan\theta_p - \tan\theta_q) \qquad (9.64)$$
$$= \frac{1}{2}\frac{f_0}{f_1 - f_2}(\tan\theta_p - \tan\theta_q) \qquad (9.65)$$

When $X = \pm R$, $\theta = \pm 45°$, which again reduces to Eq. (9.47).

To summarize, this method is used as follows: The detuned-short position is found, the cavity tuned to resonance, and the value of the coupling coefficient β measured by finding the VSWR r_0 at resonance. Additional measurements of VSWR and phase are then made at two other frequencies (which are also measured), and at as many other frequencies as are considered necessary for accuracy. Referring the measured impedances to the detuned-short position, the impedance locus is plotted together with the construction lines necessary to identify the half-power points, as shown in Fig. 9.10. The intersection of the impedance locus with the construction lines identifies the three half-power points whose frequencies can be found from the auxiliary linear-frequency scale and the construction shown in Fig. 9.11. Alternatively, the measured impedance can be referred to the detuned-open position and the VSWR and phase information transformed into data suitable for plotting in the rectangular impedance chart. The experimental points will lie along a straight line perpendicular to the resistive axis; the intersection of this locus with the construction lines shown in Fig. 9.12 locates the ordinates which correspond to the three half-power points. Since the vertical scale is linear in frequency, the ordinate intervals can be transformed into the units of frequency using the scale calibration provided by the experimental points.[1]

b. The Standing-wave Ratio Method. The method for interpreting the impedance data, described in the preceding section, is the most accurate of the three discussed in this section. However, it is time-consuming because it requires the measurement of phase and VSWR at each frequency as well as subsequent calculations to convert the laboratory data for plotting in the impedance plane. This can be simplified substantially by recording only the VSWR data as a function of frequency. Accuracy is not sacrificed by this simplification because a considerable quantity of data can be taken in a short time.

The experimental data required for the determination of Q values con-

[1] It is possible to improve the accuracy of the linear-frequency scale by arithmetically averaging the frequency intervals or by plotting the linear distance X vs. frequency and graphically finding the average slope.

sist of the plot of VSWR as a functional frequency and the value of the coupling coefficient β which is found as described in Sec. 9.3a by exploring the standing-wave pattern at the detuned-short position with the cavity tuned to resonance. Using this information, the Q values are determined as follows:

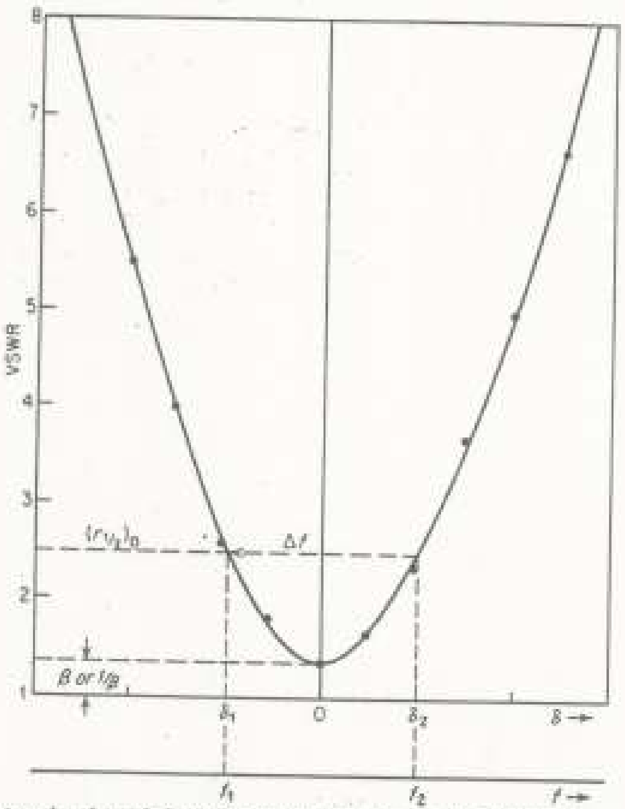

FIG. 9.13. Determination of the half-power points from the VSWR data. $r_{1/2}$ points are computed from Eqs. (9.66), (9.67), and (9.68) for Q_0, Q_L, and Q_{ext}, respectively. The curve shown represents typical data for f_0 = 3,000 Mc, Q_0 = 2,180, β = 0.76.

The variation of the input impedance of a cavity resonator referred to the detuned-short position is shown in Fig. 9.6. It can be seen that the radius vector measured from the center of the Smith chart, corresponding to the reflection coefficient, increases continuously with the frequency-tuning parameter δ. Figure 9.13 shows the typical variation of VSWR with frequency. To find the Q values, it is necessary to identify the specific values of the standing-wave ratio which correspond to the half-power points. These can be found either graphically or analytically.

The standing-wave ratios at half-power points, $(r_{1/2})_0$, $(r_{1/2})_L$, $(r_{1/2})_{ext}$, corresponding to Q_0, Q_L, and Q_{ext}, respectively, can be found graphically, using the construction shown in Fig. 9.10, which is included for clarity in Fig. 9.14. The known value of β [see Eqs. (9.41) and (9.42)] establishes the intercept between the circular impedance locus and the resistive axis, thus permitting the circle to be drawn. The construction lines corresponding to Q_0, Q_L, and Q_{ext} loci can be drawn which define the impedances at the three half-power points. The VSWR corresponding to these

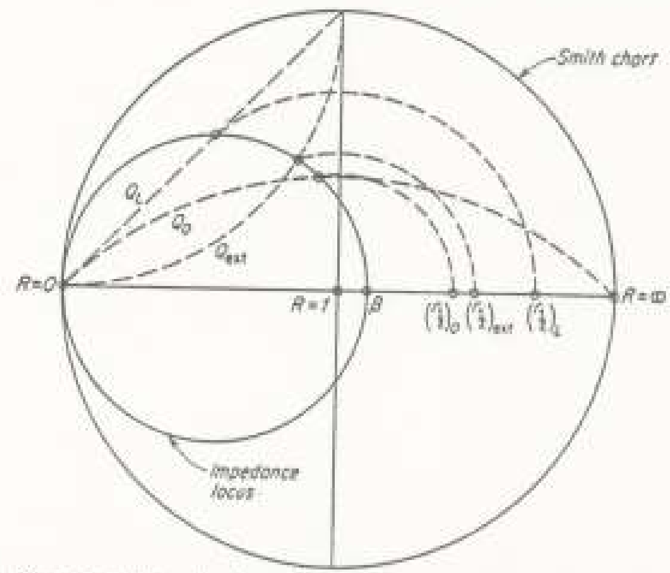

FIG. 9.14. Graphical determination of the half-power VSWR's. The experimental value of β locates the circular impedance locus; its intersection with the half-power construction lines determines the half-power VSWR values by projection to the resistive axis as indicated.

are found by drawing the dashed circular arcs, as indicated, and reading their intercept along the resistive axis.

To obtain greater accuracy, it may be desirable to find the half-power VSWR points analytically. The input impedance at the detuned short at the frequencies given by Eqs. (9.44), (9.50), and (9.51) are given by Eqs. (9.43), (9.54), and (9.55), respectively. The half-power values of VSWR at these frequencies can be found by substituting these impedance values into Eq. (4.70), giving

$$\text{For } Q_0: \qquad (r_{1/2})_0 = \frac{2 + \beta^2 + \sqrt{4 + \beta^4}}{2\beta} \tag{9.66}$$

$$\text{For } Q_L: \qquad (r_{1/2})_L = \frac{1 + \beta + \beta^2 + (1 + \beta)\sqrt{1 + \beta^2}}{\beta} \tag{9.67}$$

$$\text{For } Q_{ext}: \qquad (r_{1/2})_{ext} = \frac{1 + 2\beta^2 + \sqrt{1 + 4\beta^4}}{2\beta} \tag{9.68}$$

The ratio of the half-power VSWR to VSWR at resonance r_0 is plotted for the three cases in Fig. 9.15. For small and large values of β, this ratio is

For $\beta \ll 1$:

$$\left(\frac{r_{1/2}}{r_0}\right)_0 = 2 \qquad \left(\frac{r_{1/2}}{r_0}\right)_L = 2 \qquad \left(\frac{r_{1/2}}{r_0}\right)_{ext} = 1 \tag{9.69}$$

For $\beta \gg 1$:

$$\left(\frac{r_{1/2}}{r_0}\right)_0 = 1 \qquad \left(\frac{r_{1/2}}{r_0}\right)_L = 2 \qquad \left(\frac{r_{1/2}}{r_0}\right)_{ext} = 2 \tag{9.70}$$

These relations show that for small β the VSWR at the half-power points for Q_0 and Q_L is twice the minimum value and can be measured easily. For Q_{ext}, however, the half-power VSWR becomes undistinguishable from the VSWR at resonance and cannot be used. For similar reasons, when β is large, Q_L and Q_{ext} can be found, but Q_0 cannot. If β is measured accurately, Q_L and Q_{ext} can be computed from Q_0 (and conversely) by using Eqs. (9.9) and (9.16).

The values of Q_0, Q_L, and Q_{ext} are found from the frequencies at which the half-power VSWR occur. Calling these δ_1 and δ_2, δ_3 and δ_4, δ_5 and δ_6, respectively,

$$Q_0 = \frac{1}{\delta_1 - \delta_2} = \frac{f_0}{f_1 - f_2} \qquad Q_L = \frac{1}{\delta_3 - \delta_4} = \frac{f_0}{f_3 - f_4} \qquad Q_{ext} = \frac{1}{\delta_5 - \delta_6} = \frac{f_0}{f_5 - f_6} \tag{9.71}$$

In summary, the method is used as follows: The detuned-short position is found, the cavity carefully adjusted to resonance, and the standing-wave pattern explored to determine whether the cavity is overcoupled or undercoupled. The VSWR r_0 at resonance is measured and the value of the coupling coefficient β calculated, using Eqs. (9.41) and (9.42), as appropriate. From Eqs. (9.66), (9.67), and (9.68), or Fig. 9.15, the VSWR at the half-power points is obtained. From the experimental

graph of the VSWR vs. frequency (such as Fig. 9.13) the frequencies corresponding to the half-power VSWR are obtained. The Q values are computed from Eqs. (9.71).

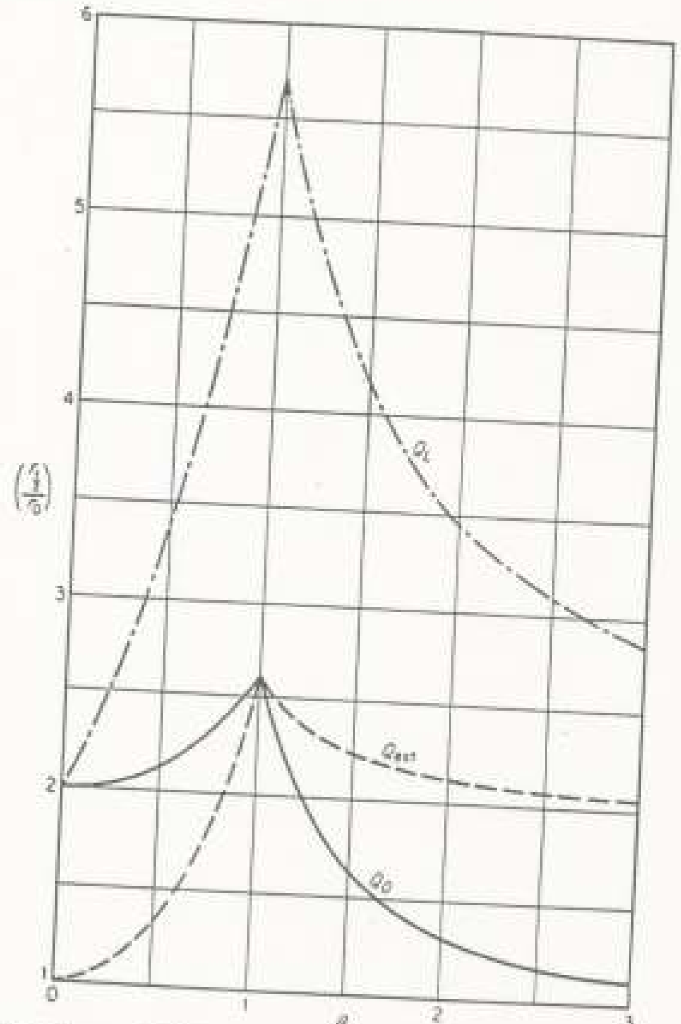

FIG. 9.15. Dependence of VSWR at half-power points upon β. $\beta = r_0$ or $1/r_0$, depending upon the degree of coupling.

c. The Phase Method. The phase method is based upon the measurement of the nodal position as a function of frequency. If $\beta \gg 1$, the standing-wave ratio is very high and difficult to measure, but the associated voltage nodes are sharp and they shift rapidly with tuning of the cavity or the source and are easily located accurately. In its basic form, the measurement of the standing-wave ratio is not needed; thus, many possible errors connected with the measurement of relative voltages, calibration of the detector-amplifier, etc., are eliminated.

The necessary laboratory data are obtained with the equipment arranged as in Fig. 9.3a. The laboratory procedure consists of tuning the cavity

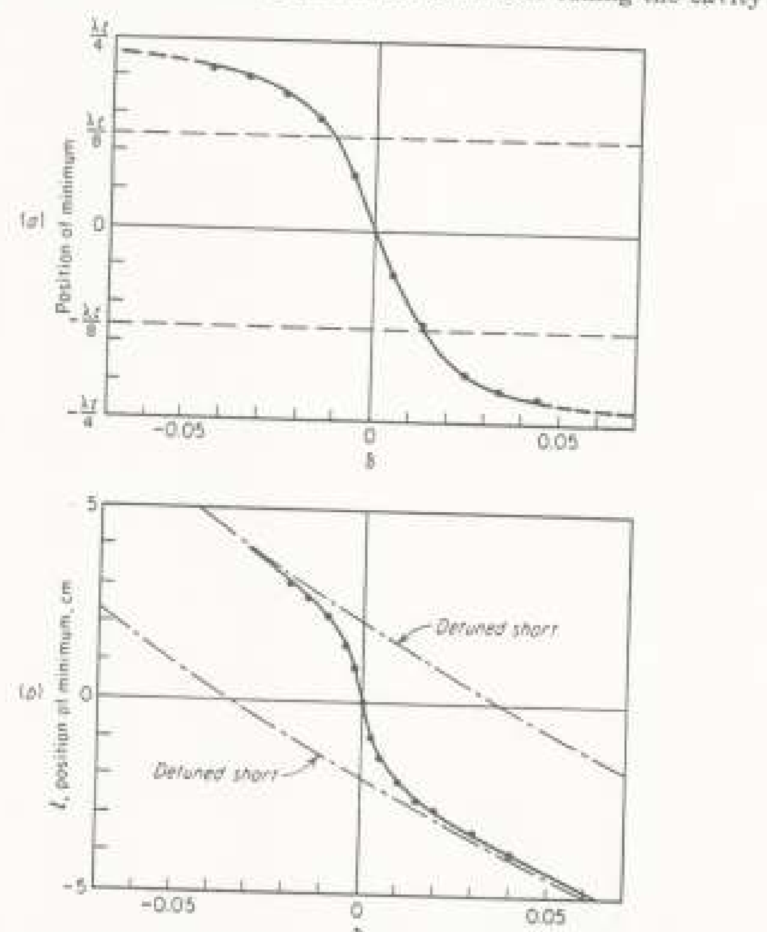

FIG. 9.16. Typical experimental data showing the displacement of the nodal position with frequency. In (a) the frequency is constant as the cavity is tuned; f_1 = 1,360 Mc, Q_{ext} = 41. In (b) the cavity tuning is constant and the frequency is varied; f_r = 9,100 Mc, Q_{ext} = 115.

or the signal source and measuring the location of voltage nodes with respect to some arbitrary reference plane; typical data are shown in Fig. 9.16. In Fig. 9.16a, the frequency is kept constant and the cavity is tuned. Except near resonance, the transmission line appears to be shorted, producing a series of voltage nodes half a wavelength apart.

As the cavity is tuned close to resonance, the positions of the nodes change; plotting the position of one of the nodes results in the curves shown. Similar data are obtained if the cavity tuning is fixed and the signal frequency is changed. A typical curve is shown in Fig. 9.16b. With the cavity tuned far off resonance, the node position changes with frequency, as indicated by the dashed lines; the slope of these depends upon the distance of the measuring probe from the cavity. With the

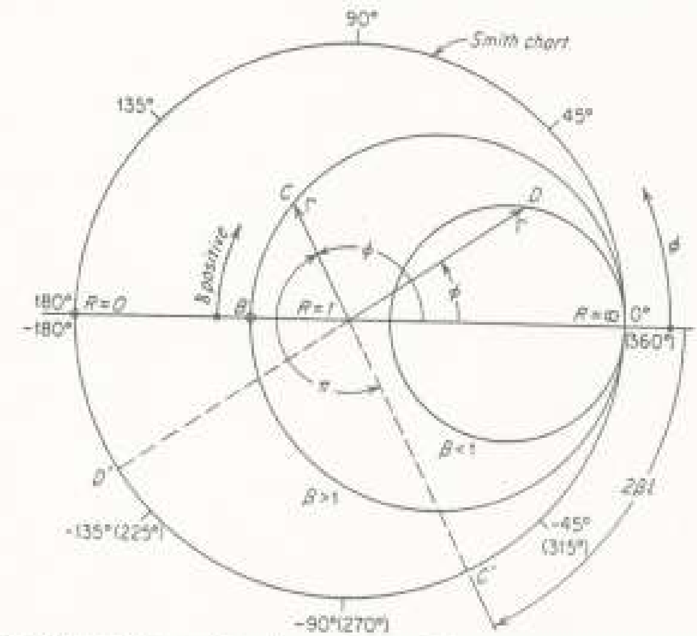

FIG. 9.17. Relation between the phase angle φ of the reflection coefficient Γ and the position of the voltage minimum.

cavity tuned to resonance, tuning the signal source through the resonance frequency of the cavity results in the curve shown. The data can be altered, if desired, to appear as shown in Fig. 9.16a by subtracting from each point a distance corresponding to the displacement of the detuned short.

In the analysis of this procedure it is convenient to use the series representation of the cavity given by Eq. (9.26). The term δ_0 is not important as it merely represents a shift along the frequency scale and is neglected for brevity. Thus, Eq. (9.26) can be written as

$$\frac{Z_{co}}{Z_0} = \frac{1}{\beta}(1 + j2Q_0\delta) \tag{9.72}$$

Figure 9.17 shows the impedance referred to the detuned-open position plotted on the Smith chart. Points A and B show the impedance at resonance for the undercoupled and overcoupled cases, respectively. The complex reflection coefficient Γ measured at a distance l from the detuned-open position is obtained by substituting Eq. (9.72) into Eq. (4.69); thus,

$$\Gamma = \left| \frac{(Z_{ee}/Z_0) - 1}{(Z_{ee}/Z_0) + 1} \right| \underline{/\phi - 2\beta l} \qquad (9.73)$$

where ϕ is the phase angle Γ at $l = 0$. For convenience, let

$$y = 2Q_0\delta \qquad (9.74)$$

Substituting Eq. (9.72) into Eq. (9.73) and rationalizing, the phase angle ϕ is

$$\phi = \tan^{-1} \frac{2\beta y}{1 - \beta^2 + y^2} \qquad (9.75)$$

At resonance ($y = 0$), from Fig. 9.17 or Eq. (9.75), the phase angle $\phi = 0$ and $\phi = \pi$ for the undercoupled and overcoupled cases, respectively.

The voltage minimum occurs when the phase angle of Γ is $n\pi$, or

$$\phi - 2\beta l = \pm n\pi \qquad (9.76)$$

or

$$2\beta l = \phi \pm n\pi \qquad (9.77)$$

with $n = 1, 3$, etc. Equation (9.77) determines the distance l between the voltage node and the detuned-open position; the phase angle ϕ is defined by the frequency through Eq. (9.75). Thus, the location of the voltage node is found from the Smith chart to be the electrical distance $2\beta l$, as indicated in Fig. 9.17.

Qualitatively, the relation between δ and the location of the voltage node can be predicted by tracing a point along the impedance locus and observing the variation in $2\beta l$. Consider the two cases illustrated in Fig. 9.17. For $\beta > 1$, at resonance, the minimum occurs at point B; as δ increases from zero to infinity, ϕ varies from π to zero. Consequently, $2\beta l$ begins at 0° and progresses through negative angles to −180°, as can be verified by tracing the motion of the point C' when C moves from B to O. When $\beta < 1$, at resonance the point A corresponds to a voltage maximum; the voltage minimum is found by adding 180°. Tracing the point D along the impedance locus as δ increases from zero to infinity causes the point D' to begin at −180°, decrease toward −90°, and return again to −180°. Figure 9.18 shows the plot of $2\beta l$ vs. the tuning parameter δ obtained by calculation from Eqs. (9.77) and (9.75) for three conditions of coupling and illustrates the data that can be obtained in the laboratory.

The characteristics of the curves shown in Fig. 9.18 depend upon Q_0 and β. For computation, the cardinal points can be selected in the following manner: The resonant frequency, $\delta = 0$, can be taken as the

point of antisymmetry. Let the slope at this point be called S_0. In the overcoupled case, let the frequencies at which the curve passes through ±90° points be called δ_1 and δ_2. In the undercoupled case the frequencies corresponding to the points of zero slope are called δ_3 and δ_4. These values are identified in Fig. 9.18.

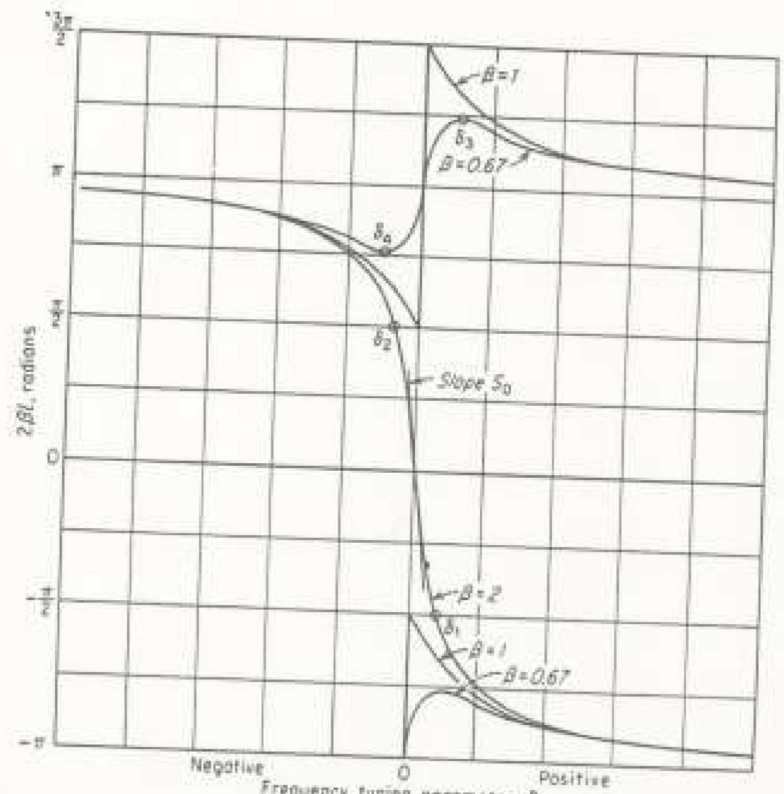

FIG. 9.18. Computed curves showing the displacement of the voltage minimum with respect to the detuned-open position. The cardinal values of δ used in the calculation of the Q values are shown.

Analytic expressions connecting the β and Q values with $\delta_1, \ldots, \delta_4$ can be found as follows: The slope of the curves shown in Fig. 9.18 can be obtained by differentiating Eq. (9.77) with respect to δ:

$$\frac{d}{d\delta}(2\beta l) = \frac{d\phi}{d\delta} = 2Q_0 \frac{d\phi}{dy} \qquad (9.78)$$

Hence, differentiating Eq. (9.75) with respect to y leads to

$$\frac{d\phi}{d\delta} = 4Q_0\beta \frac{1 - \beta^2 + y^2}{(1 - \beta^2 + y^2)^2 + (2y\beta)^2} \qquad (9.79)$$

At resonance,

$$S_0 = \frac{d\phi}{d\delta}\bigg|_{\delta=0} \tag{9.80}$$

$$S_0 = \frac{4Q_0\beta}{1-\beta^2} \tag{9.81}$$

In the undercoupled case the points of zero slope are found from Eq. (9.79) by equating the numerator to zero. These occur at

$$\begin{aligned} 2Q\delta_4 &= \sqrt{1-\beta^2} \\ 2Q\delta_3 &= -\sqrt{1-\beta^2} \end{aligned} \tag{9.82}$$

In the overcoupled case the curve passes through the points $\pm 90°$ at which $2\beta l = \pm\pi/2$. Therefore, from Eq. (9.77), this occurs when $\phi = \pi/2$. Hence, $\tan\phi = \infty$; this occurs when the denominator in Eq. (9.75) is zero. This leads to

$$\begin{aligned} 2Q\delta_1 &= \sqrt{\beta^2-1} \\ 2Q\delta_2 &= -\sqrt{\beta^2-1} \end{aligned} \tag{9.83}$$

Equations (9.81), (9.82), and (9.83) contain the necessary information to evaluate the cavity parameters. Solving these for Q_0 and β results in

Undercoupled case ($\beta < 1$):

$$\beta = \frac{\delta_3 S_0}{2\sqrt{(\delta_3 S_0/2)^2+1}} \tag{9.84}$$

$$Q_0 = \frac{1}{2\delta_3\sqrt{(\delta_3 S_0/2)^2+1}} \tag{9.85}$$

Overcoupled case ($\beta > 1$):

$$\beta = \frac{S_0\delta_1}{2\sqrt{(S_0\delta_1/2)^2-1}} \tag{9.86}$$

$$Q_0 = \frac{1}{2\delta_1\sqrt{(S_0\delta_1/2)^2-1}} \tag{9.87}$$

$$Q_{ext} = \frac{Q_0}{\beta} = \frac{1}{S_0\delta_1{}^2} \tag{9.88}$$

$$Q_L = \frac{Q_0}{1+\beta} = \frac{1}{2\delta_1[\sqrt{(S_0\delta_1/2)^2-1}+(S_0\delta_1/2)]} \tag{9.89}$$

If $\beta \gg 1$, from Eq. (9.81), $S_0 = 4Q_0/\beta$, or

$$Q_{ext} = \frac{S_0}{4} \tag{9.90}$$

Alternatively, combining Eqs. (9.88) and (9.90), for $\beta \gg 1$,

$$Q_{ext} = \frac{1}{2\delta_1} \tag{9.91}$$

or

$$Q_{ext} = \frac{1}{\delta_2-\delta_1} = \frac{f_0}{f_1-f_2} \tag{9.92}$$

Equating Eqs. (9.90) and (9.91) shows that the quantity $S_0\delta_1$ is approximately equal to 2 for the overcoupled case. An examination of Eqs. (9.86) through (9.89) shows that the denominators contain the difference of two nearly equal numbers. For this reason, the values of β and Q_0 cannot be accurately determined by this method, although it is accurate for measuring Q_{ext}. For the undercoupled case, the method is

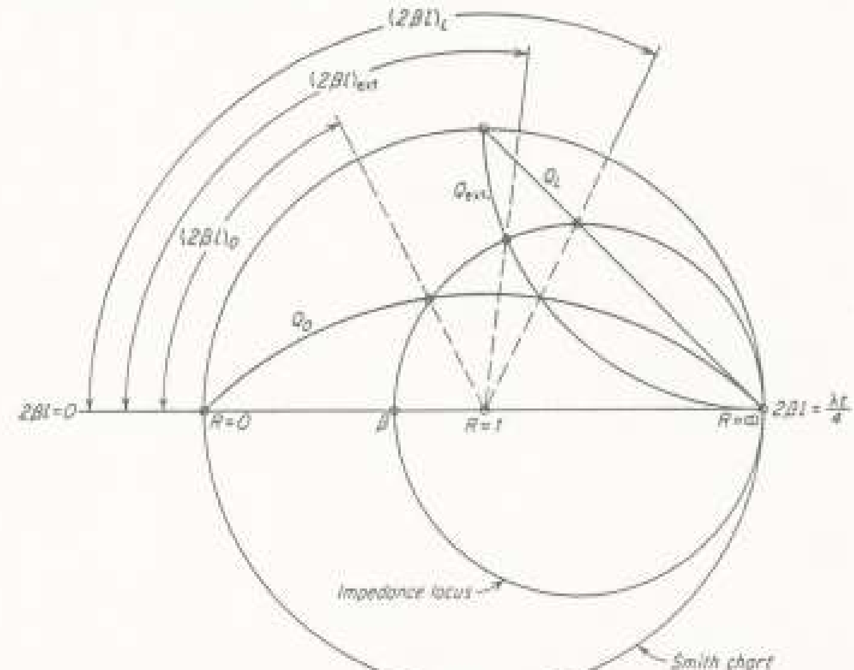

FIG. 9.19. Determination of the voltage node displacements $2\beta l$ corresponding to the half-power points for Q_0, Q_L, and Q_{ext}. The circular impedance locus is drawn through the experimental value of β.

not as useful as the VSWR method described in Sec. 9.3b, since it is difficult to find accurately the location of the minima due to their breadth at low VSWR; also, for $\beta \ll 1$, the minima do not shift sufficiently for accurate measurement.

To summarize, this method is used as follows: With the cavity tuned far from resonance, a location of a voltage node is found. As either the cavity or the signal source is tuned toward resonance, the position of the node changes. A graph showing the node position vs. the tuning parameter δ is plotted using the coordinate axes shown in Fig. 9.18. Using Eqs. (9.86) through (9.92), as appropriate, the Q values can be computed.

This method can be modified by measuring the VSWR at resonance. The displacement of the voltage node at the frequencies corresponding to the three half-power points can be found graphically from the construction lines shown in Fig. 9.10. These are repeated for convenience in Fig. 9.19, which shows the nodal displacements explicitly. The measured value of β at resonance establishes the intercept of the impedance locus with the resistive axis and permits the circle to be drawn. The intersection of the construction lines with the impedance locus determines the displacement of the voltage node at the half-power frequencies.

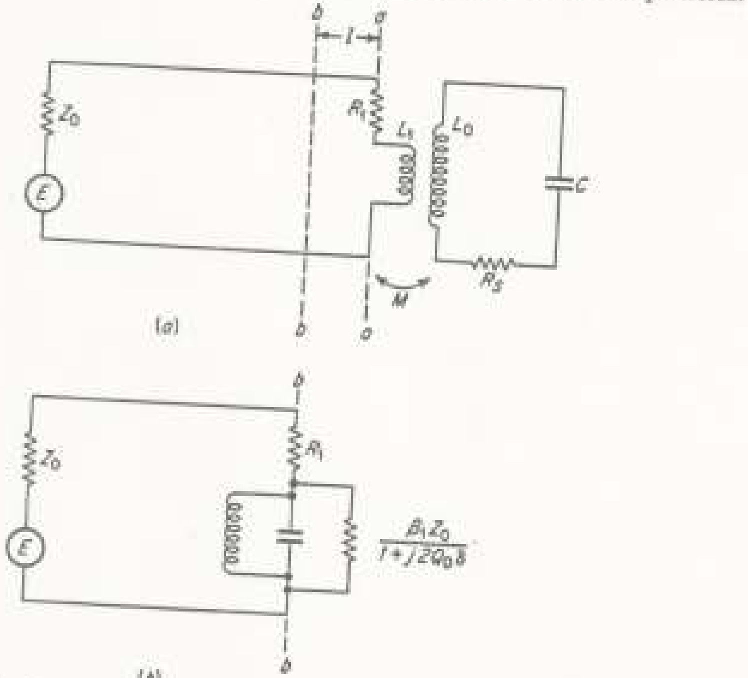

FIG. 9.20. Equivalent circuit used in the analysis of the effect of the coupling loss. (a) Equivalent circuit of the coupling system, (b) referred to the detuned-short position, b-b.

From the experiment graph of V_{min} vs. frequency, shown in Fig. 9.16, the frequencies corresponding to these displacements are found and the Q values computed using Eqs. 9.71.

9.4. Impedance Method—Effect of Coupling Loss. The three impedance methods for measuring the Q values, described in Sec. 9.3, are based upon the assumption that the cavity coupling network is lossless. In most practical cases this approximation is valid; however, if losses are present, the impedance methods presented cannot be applied directly and must be altered. For brevity, only the modification of the VSWR method is considered in detail, but the method of analysis can be extended to the remaining cases as well. It should be noted that the definitions

of the loaded and external Q values are also modified by the presence of loss.[1]

Figure 9.20a is the equivalent circuit of a cavity coupled to the transmission line and corresponds to Fig. 9.3b with the addition of the series resistance R_1. It is assumed that the loss in the coupling element can be represented in this manner regardless of the actual cause of loss. The input impedance as a function of frequency results in a circular locus as

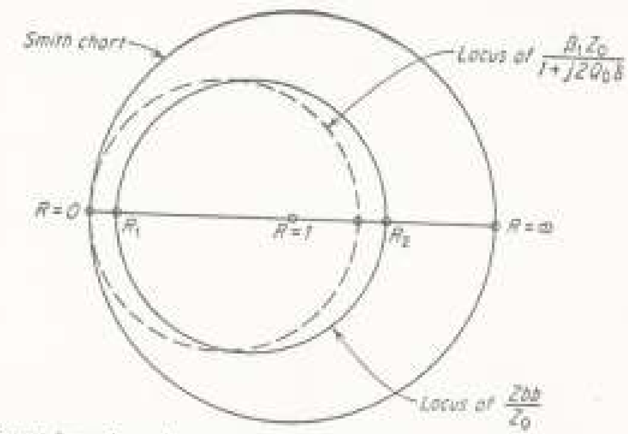

FIG. 9.21. Input impedance locus of a resonance cavity in the presence of loss in the coupling network.

shown in Fig. 9.21. The plot of VSWR vs. frequency is shown in Fig. 9.22. The characteristic feature of the two graphs is the fact that the VSWR far off resonance reaches a limiting value, r_{min}, instead of becoming infinite.

Qualitatively, the impedance information is interpreted as in the former case. Certain points on the impedance locus are found which correspond to the half-power points and the frequency interval between them defines Q_0. Due to the coupling loss, the identification of the half-power points is somewhat different from the lossless case. The desired relations between the characteristic points of the impedance locus and the frequencies corresponding to the half-power points can be obtained in the following manner:

Referring to Fig. 9.20a, the impedance at a-a is

$$\frac{Z_{aa}}{Z_0} = \frac{R_1 + jX_1}{Z_0} + \frac{\beta_1}{1 + j2Q_0\delta} \qquad (9.93)$$

With the cavity tuned far off resonance, the transmission line is terminated by the self-impedance of the coupling element. As before, using

[1] L. Malter and G. R. Brewer, Microwave Q Measurements in the Presence of Series Losses, *J. Appl. Phys.*, vol. 20, no. 10, pp. 918-925, October, 1949.